RESIDUAL STRESS RELAXATION OF QUASI-STATICALLY AND CYCLICALLY-LOADED STEEL WELDS

M. Farajian-Sohi

Th. Nitschke-Pagel

K. Dilger

ABSTRACT

Weld fatigue strength is currently the bottleneck to designing high performance and lightweight welded structures using advanced materials. In addition to loading conditions, environmental aspects, geometrical features and defects, it has been proven that studying the influence of residual stresses on fatigue performance is indispensible. The extent of the influence is, however, a matter of discussion. In this work, residual stress behaviour in welded S355J2G3 and S1100QL steel specimens under quasi-static and cyclic loading were studied and the correlation between the relaxation of residual stress field and mechanical properties was studied. Residual stress measurements were performed using the X-ray diffraction technique. The relaxation behaviour in S355J2G3 at weld metal, weld toe and in the base metal could be described by Von Mises criteria. This was not the case for S1100QL. In the case of relaxation, it was observed that if the Von Mises stress, as a function of residual, load and mean stresses, exceeds the monotonic yield strength of the base metal, relaxation takes place. Otherwise, the internal elastic stresses remain stable regardless of the number of loading cycles and could contribute to fatigue damage.

IIW-Thesaurus keywords: *Fatigue strength; Mechanical properties; Reference lists; Residual stresses; Stress; Welded joints.*

INTRODUCTION

Residual stresses and fatigue of welds

The extent of the influence of residual stresses on the fatigue strength of welded structures is a matter of discussion. Some researchers overlook this influence in the case of high quality welds [1, 2]. Others recognize the significance of the effects of residual stresses on fatigue strength [3]. The uncertainty of residual stress effects on fatigue is based on the lack of insight into their behaviour under loading. Residual stresses are blamed for causing failures whenever an acceptable explanation for the failure cannot be given. These stresses are sometimes neglected due to relaxation under repeated loading, but so far little information is available about the redistribution of the welding residual stress field under different types of loading (e.g. thermal, static, cyclic and impact). There is also few literature available concerning the influence of this redistribution on fatigue crack growth rate and propagation. In spite of the lack of knowledge about welding residual stress behaviour under loads, there is a tremendous amount of research concerning post-weld improvement techniques. These techniques induce compressive residual stresses at the most common sites for service fatigue failure in order to increase the fatigue performance of the joints [4]. This is done either mechanically (e.g. shot peening, hammer peening, needle peening, ultrasonic peening, autofretage, hole expansion, laser shock peening, low plasticity burnishing) or by influencing the phase transformation during solidification of the weld

Mr. Majid FARAJIAN-SOHI (m.farajian@tu-bs.de), M.Sc., Dr.-Ing. Thomas NITSCHKE-PAGEL (t.pagel@tu-bs.de) and Univ.-Prof. Dr.-Ing. Klaus DILGER (k.dilger@tu-bs.de) are with the Institute of Joining and Welding, University of Braunschweig, Braunschweig (Germany).

Doc. IIW-1980-08 (ex-doc. XIII-2219r1-08), recommended for publication by Commission XIII “Fatigue of Welded Components and Structures.”

pool (e.g. using Low Temperature Transformation (LTT) electrodes and introducing compressive residual stresses to the weld toe) [5, 6].

In this work, the relaxation behaviour of welded S355J2G3 and S1100QL steel specimens in three different welding zones, namely, weld metal, toe and base metal, is studied. The mechanical properties in all of the investigated welding zones are assumed to be similar to that of the base material. The influences of stress concentration at the weld toe and stress reduction in the weld metal are considered in the calculations.

Residual stress relaxation in welds

Residual stresses can be relaxed by supplying sufficiently high amounts of thermal and/or mechanical energy, which transforms the residual elastic strains to micro-plastic strains [7]. The transformation mechanism could be a combination of dislocation slip, dislocation creep, grain boundary slip and diffusion creep [8]. Despite considerable research, the technical challenge of understanding and accurately quantifying residual stress relaxation and redistribution under cyclic, mechanical and thermal loads, persists [9]. Cyclic residual stress relaxation has been observed many years ago by Mattson and Coleman [10]. Some of the first works on prediction of residual stress, based on mean stress relaxation, were carried out by Morrow and Sinclair [11] in axial fatigue tests. Jhansale and Topper [12] suggested a logarithm linear relationship between mean stress relaxation and axial, strain-controlled cycles.

The majority of recent research work dealing with residual stress relaxation has focused on shot-peened samples. Many of these works, according to [7], deal with the thermal relaxation of residual stresses [13-22], as well as quasi-static relaxation [23-27] and cyclic relaxation [28-39] at room temperature. Residual stress relaxation modelling has been investigated in some of these studies. In his work, Kodama [29] observed a considerable decrease in the compressive residual stresses induced by shot peening on annealed carbon steel. He divided the relaxation during fatigue loading into two stages: the surface yielding in the first cycle and gradual changes in the following cycles. The experimental data support the linear logarithmic decrease relationship between residual stress and load cycles, only after the first cycles. The stress ratio was not considered in this model. Holzapfel *et al*. [7] studied the relaxation of residual stress in shot-peened AISI 4140 steel under quasi-static and cyclic loading at high temperatures. In this work, the relaxation is divided into three stages: firstly, the relaxation in the first half-cycle, which could be discussed on the basis of the effects due to quasi-static loading. Secondly, the relaxation which takes place between the first cycle (N = 1) and the number of cycles to crack initiation N_i. The relation between the residual stress and the logarithm of N in this phase is linear. Thirdly and finally, for $N > N_i$, the residual stress reduction with the logarithm of N is stronger than linear. There are also some studies done by analytically modelling the relaxation by means of finite element analysis [39].

So far, the residual stress behaviour of welded joints and components under loads has attracted insufficient attention. In contrast to the shot peening process, in which the residual stress has a uniform distribution field, the welding-induced residual stress field has non-uniform characteristics with maxima and minima. Secondly, the material experiences local metallurgical changes in the weld and its vicinity. These two factors make the investigation of welding residual stress relaxation and behaviour more complicated.

EXPERIMENTAL WORK

Experimental assessment of residual stresses

Investigating the whole weld residual stress field and its relaxation during mechanical loading would provide a deeper insight into material behaviour at the cost of time and technical complexity. In this work, the surface and sub-surface residual stresses were studied, since the onset of fatigue damage almost always occurs at the surface and studying the residual stress behaviour at crack initiation sites would give some hints about the influence of residual stress behaviour on the fatigue performance of welds.

Based on the X-ray diffraction technique, residual stress measurements were taken by a middle point free 8-axis diffractometer. By the X-ray diffraction technique, the residual stress can be measured in the surface layer at a depth of 20 μm and by analysing the X-ray intensity peaks, the degree of cold work and cyclic softening can be studied. Thus, X-ray diffractometry offers a means of studying the inter-dependent processes of residual stress relaxation and cyclic deformation, as well as the characteristics of material hardening and softening. By using Cr-Kα radiation (35 kV, 30 mA), the interference line from {211} ferrite lattice plane under seven Ψ angle (0°, 9°, 18°, 27°, 33°, 39° and 45°) for 2θ between 149 and 163 were registered by a position-sensitive detector (PSD), which allows the registration of complete interference lines at a glance. The diameter of the measurement spot was 2 mm. The measurement spots were chosen on a line perpendicular to the welding direction (Figure 1). On this line, residual stress measurement was performed in transverse and longitudinal directions. For the stress evaluation, the $\sin^2\Psi$ [40] method was used. The method used to determine the peak position of the interference lines was the centre of gravity. Residual stress analysis using X-ray has been explicitly described in [41].

Welding process and welding parameters

Welding residual stresses in welded specimens in the initial state and after quasi-static and cyclic loading were measured and the behaviour of the residual stresses under loading was investigated. Steel plates

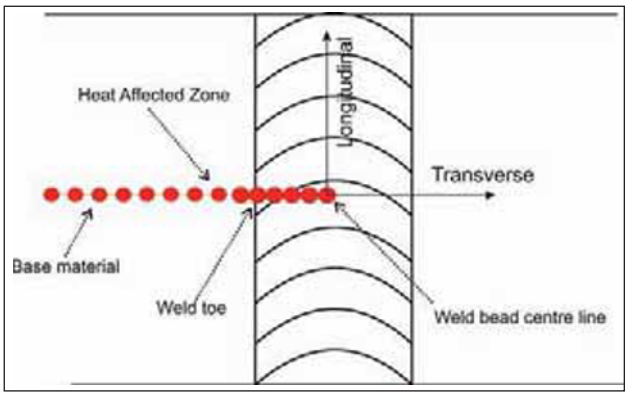

Figure 1 – X-ray diffraction measurement points on a line perpendicular to the welding direction

(400 x 200 x 6 mm) were prepared from S355J2G3 and S1100QL. For producing the S355J2G3 specimens, the TIG welding process with filler wire was used to weld every two of the steel plates, applying four single pass vee-groove welds. The heat input of each welding pass was adjusted to between 6.5 and 7.7 kJ/cm and no preheating of the plates was done (Table 1).

For S1100QL samples, the TIG process without filler wire was used to melt the plate and produce bead-on-plate welds. After melting and solidification, the plates were then sliced into smaller plates and final specimens were produced by machining [Figure 2 a)].

It is noteworthy to mention that during the slicing and machining of the plates to their final dimension, the residual stresses relax partly. Depending on the cutting location on the plates, specimens with slightly different residual stress fields are produced. Therefore, the specimens have been treated individually and the initial residual stress has been measured in every specimen before applying the load.

Quasi-static and cyclic loading of the welded specimens

In order to study the influence of quasi-static tension and compression, as well as cyclic loading on the alteration of initial residual stresses, a servo-hydraulic testing machine (Walter & Baiag: 250 kN) was used. For quasi-static loading, after each tensile or compression loading step, the residual stresses were measured by means of X-ray diffractometry. The loadings and measurements were performed until no considerable variation in the residual stress field was observed, or the nominal stress in the specimen reached the ultimate tensile strength of the base metal.

In cyclic loading, after the first half-cycle, the loading was stopped, followed by measurement of the residual stress, after which the loading was stopped after 1, 10,

Table 1 – Welding parameters used in this study for welding S355J2G3 plates

Parameter	Weld passes			
	Pass 1	Pass 2	Root pass	Cover pass
Voltage [V]	12	12	12	14
Start current [A]	20	20	20	20
Background current [A]	150	150	150	190
Pulsed current [A]	150	210	210	270
Transition current [A]	140	140	140	230
End current [A]	100	100	100	10
Background time [ms]	25	4	4	4.5
Pulse duration [ms]	25	4	4	4.5
Ramp duration [ms]	0.2	1	1	1
Welding speed [cm/min]	14	18	18	18
Wire feed speed [cm/min]	30	70	30	90
Heat input [kJ/cm]	7.7	7.2	7.2	6.5
Gas flow rate (Ar) [l/min]	10	10	10	10

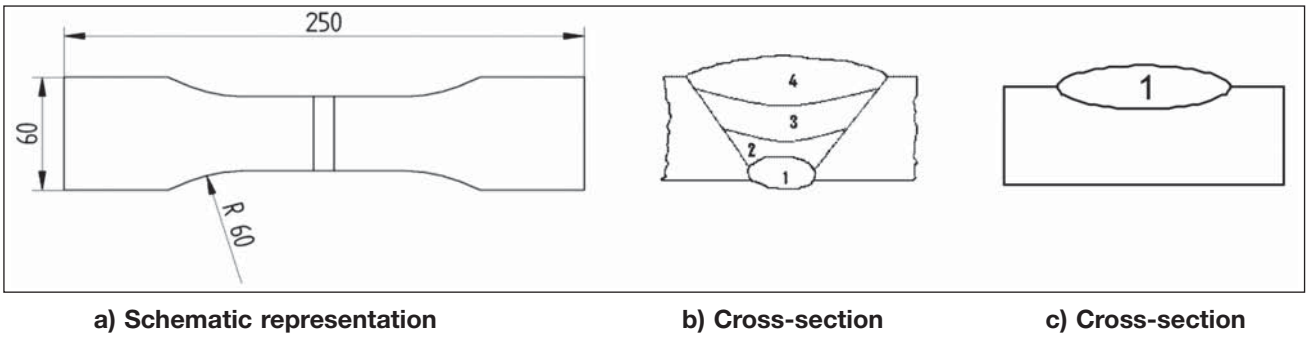

a) Schematic representation of the welded specimens **b) Cross-section of S355J2G3** **c) Cross-section of S1100QL**

Figure 2

10^2, 10^3, 10^4 number of cycles and the X-ray measurement was performed.

OBSERVATION

Residual stress distribution after welding in S355J2G3 and S1100QL

The fatigue crack initiation sites in welds are notches at the weld toe and root, even if higher tensile residual stresses are found mostly in the weld seam. In order to understand the relaxation mechanisms, the residual stress distribution and its relaxation under loads in the weld metal, the heat-affected zone and the base material were investigated. The representative distribution of transverse and longitudinal residual stresses on the sub-surface of the S355J2G3 and S1100QL steel specimens are illustrated in Figures 3 and 4. The full-line curves present the average of the residual stress values of 15 specimens, measured along the measure line (Figure 1) in transverse and longitudinal directions. The dashed lines and the area in-between illustrate the scatter band of the measured residual stresses.

The transverse residual stress distribution in Figure 3 a) shows a maximum value of 200 MPa at the weld centre line. From this point to the weld toe, the tensile, transverse, residual stress profile increases until it reaches its maximum value in the vicinity of the weld toe, after which it decreases with a relatively high gradient through the heat-affected zone and reaches a value of –100 MPa. Thereafter, it rises a little in value in the base material, with a distance 8 to 12 mm from the weld centre line and then it decreases to its minimum of –150 MPa in the base material. The longitudinal, residual stress distribution, on the other hand, shows low tensile, residual stresses of 35 MPa on the weld centre line. From this point to the weld toe, the longitudinal, residual stress reaches a maximum value of 60 MPa shortly before the weld toe. This profile experiences a minimum shortly after the weld toe in the heat-affected zone and reaches the same level of tensile residual stress as in the weld centre line. In contrast to the steep decrease of transverse residual stress in the heat-affected zone, the longitudinal residual stress shows no significant changes. From the heat-affected zone to the base material, the residual stress profile experiences its maximum value at a distance of 10 mm

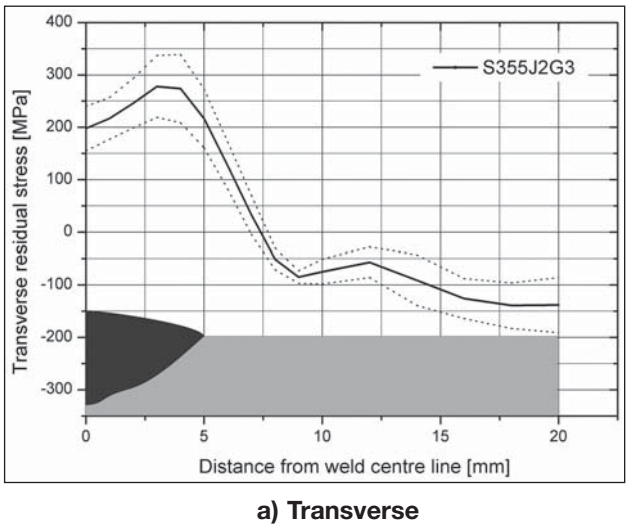

a) Transverse

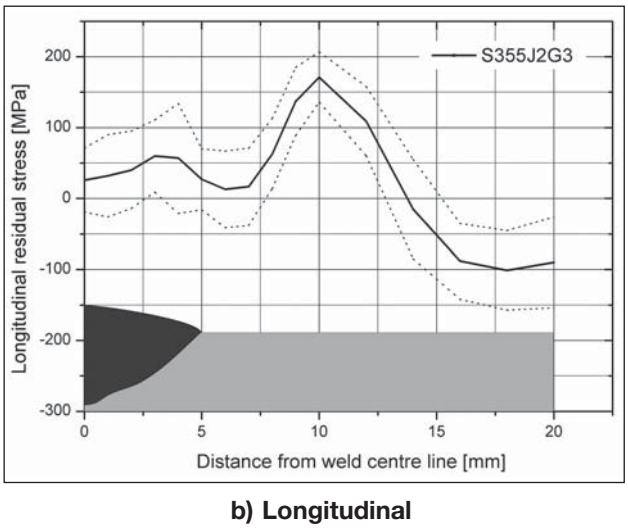

b) Longitudinal

Figure 3 – Residual stress distribution in S355J2G3 specimens

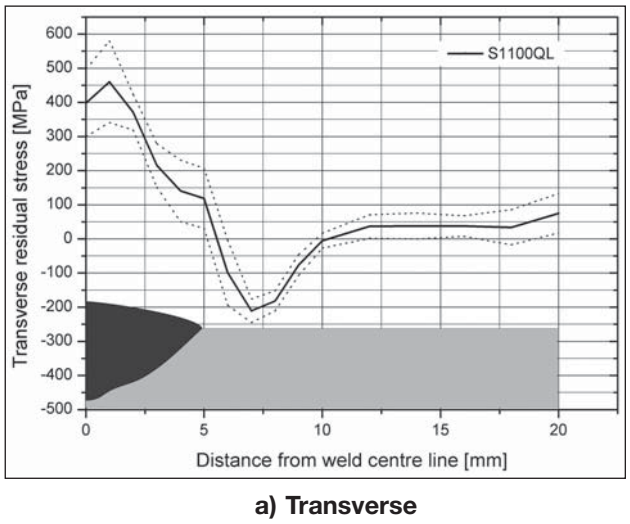

a) Transverse

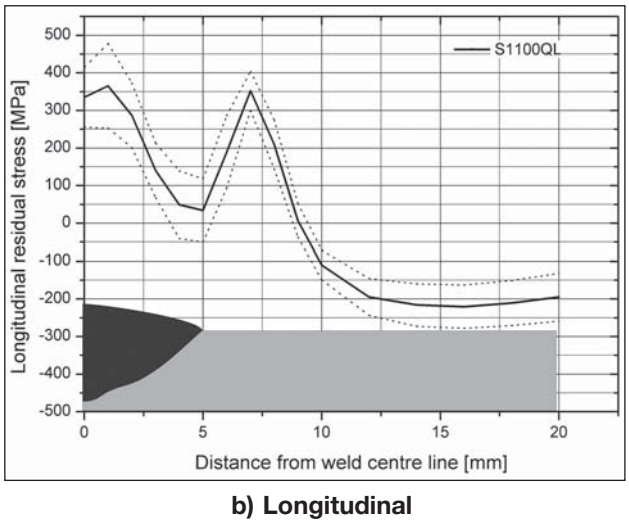

b) Longitudinal

Figure 4 – Residual stress distribution in S1100QL specimens

from the weld centre line, whereafter it decreases again to a value of –100 MPa.

In Figure 4, the transverse and longitudinal, residual stress profiles in the S1100QL specimens show relatively larger values, compared to those of the S355J2G3 specimens. The transverse residual stress at the weld centre line has a value of 400 MPa. After a small increase and having reached its maximum value of 450 MPa, the stress profile decreases moving toward the base metal. At the weld toe it reaches 120 MPa, after which it drops to its minimum of –200 MPa. The steep slope of the transverse, residual stress curve in the heat-affected zone was also observed in the S355J2G3 specimens. The stress curve subsequently rises to a value of 50 MPa and then remains without considerable changes throughout the base metal. The longitudinal, residual stress curve starts with 340 MPa at the weld centre line and after a small rise, decreases to a minimum at the weld toe with 40 MPa. It then increases to a maximum of 350 MPa through the heat-affected zone, whereafter it decreases with a high gradient to its minimum of –200 MPa and remains constant throughout the base metal.

Residual stress relaxation and behaviour under static tension loading

To study the relaxation in S355J2G3 and S1100QL welded specimens under tensile loading, specimens with already-measured residual stress were chosen. The specimens were then loaded, unloaded and investigated by means of an X-ray diffractometer. The loading was stopped when no considerable changes in the residual stress profile could be observed.

After the first loading with a nominal stress of 100 MPa, it can be seen in the S355J2G3 welded specimen [Figure 5 a)] that the transverse residual stress profile is relaxed along the measure line from the weld centre line to the weld toe. At the weld toe, the initial, tensile residual stress after loading changes signs and amounts to –50 MPa. In the heat-affected zone, the compressive residual stress increases in the negative direction and the maximum peak of –200 MPa reaches –350 MPa. In the base material, at the distance of 10 mm from the weld centre line, tensile residual stress of 100 MPa is almost relaxed to zero value. By further loading the specimen, the transverse residual stress relaxes in the tension and compression fields. At the weld centre line, it diminishes to 90 MPa and at the minimum in the heat-affected zone, it increases to –280 MPa. At the weld toe it ends up at –100 MPa.

For S1100QL, the behaviour of the transverse residual stress is almost the same. In the weld and base material, the sub-surface, initial residual stress is tensile and in the heat-affected zone, it is compressive. After loading the specimen up to a nominal stress of 1 000 MPa, the residual stress in the tension and compression fields relaxes. At the weld centre line, it relaxes from the initial value of 700 MPa to 190 MPa. At the weld toe, the residual stress takes its initial value of 100 MPa after a small alteration during loadings. In the heat-affected zone and base metal, the compressive residual stress changes signs and becomes positive.

Residual stress relaxation and behaviour under cyclic loading

Cyclic loading of the specimens was done with and without the application of mean stresses. It was observed that in the case of a relaxation, the first half-cycle plays a significant role. In Figure 6, the relaxation of transverse residual stress of a S355J2G3 specimen under cyclic loading, with amplitude of 300 MPa and without mean stress, is observed. The initial residual stress in black, with a maximum value of around 350 MPa at the weld centre, decreases moving toward the weld toe, followed by a steep reduction through the heat-affected zone, whereafter it increases again in the base metal. After the first half-loading, i.e. increasing the load to 300 MPa and re-loading the specimen, the transverse residual stress profile experiences a large relaxation. In the weld centre line, it relaxes to 250 MPa and at the weld toe, it reduces from 100 MPa to zero. In the heat-affected zone and the base metal, with compres-

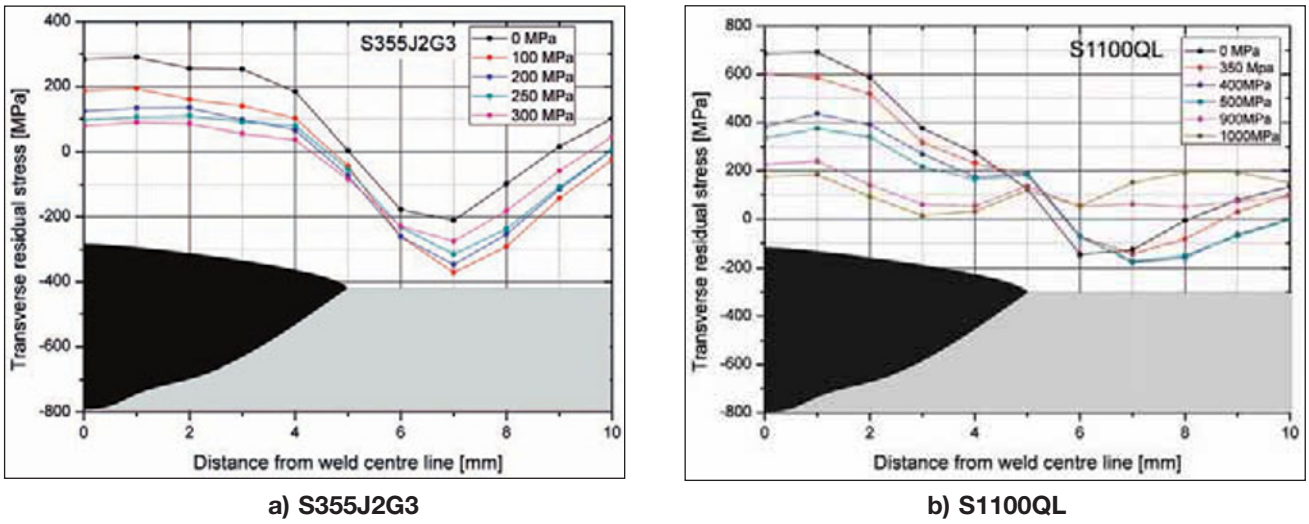

a) S355J2G3 **b) S1100QL**

Figure 5 – Transverse residual stress relaxation under quasi-static loading

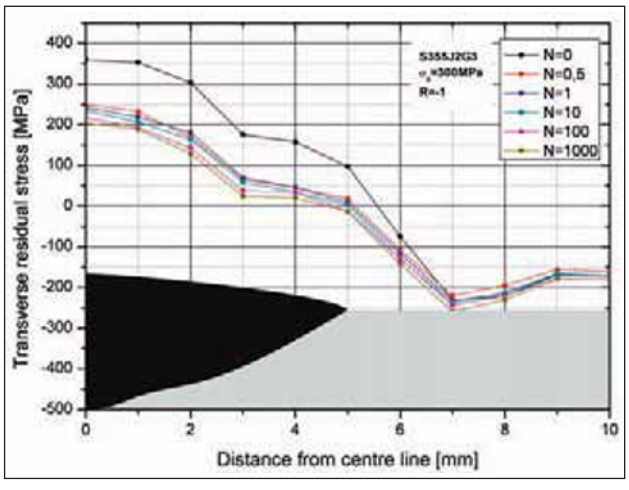

a) with S355J2G3

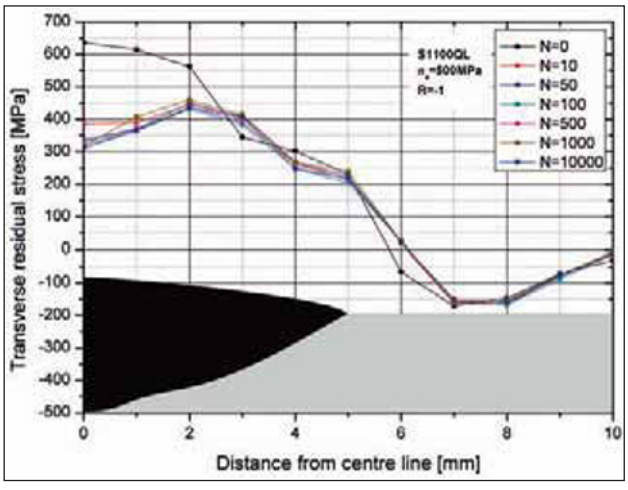

b) with S100QL

Figure 6 – Residual stress relaxation under cyclic loading

sive residual stresses, little changes are observed. By further loading the specimen up to 1 000 cycles, slight changes of the stress profile could be observed.

For the S1100QL welded specimen, the behaviour is the same as for the S355J2G3. In the first cycles, the transverse residual stress in the weld centre line and its vicinity reduces considerably, whereafter no changes are observed, in spite of cyclically loading the specimen 10 000 times with 500 MPa load amplitude. In the weld centre line, the transverse residual stress before loading amounts to 640 MPa. Within the first 10 cycles, it reduces to 390 MPa. At the weld toe, no changes of the stress value before and after loading is observed. In addition, in the heat-affected zone and base metal, the residual stress profile stays constantly in compression.

MECHANICAL AND METALLURGICAL CHARACTERIZATION

In order to investigate the behaviour and mechanisms of the welding residual stress relaxation under static and cyclic loadings in different welding zones, mechanical and metallurgical characteristics of the materials used in this work were determined. The analysis is based on the assumption that the yield strengths in different welding zones are similar to the yield strength of the base metal.

Base material characterization

The static and cyclic mechanical properties of S355J2G3 and the static properties of S1100QL were evaluated using tensile and multiple step tests, respectively. For the static mechanical properties, the specimens and the procedures were chosen according to the ASTM standard 8E – test methods for tension testing of metallic materials. For the cyclic behaviour and determination of stress-strain properties with reversal load, however, there is no procedural standard. Since the cyclic stress strain tests are accomplished in a similar manner to low cycle fatigue endurance tests, the ASTM – 606-92, which is standard practice for strain-controlled fatigue testing, was used as the base code of practice.

Figures 7 a) and b) show the monotonic, stress-strain curve of the base metals used in this investigation. Table 2 summarizes the results of the mechanical testing

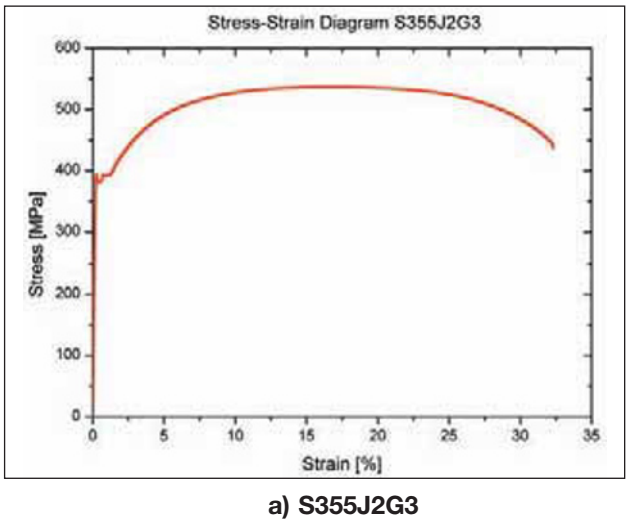

a) S355J2G3

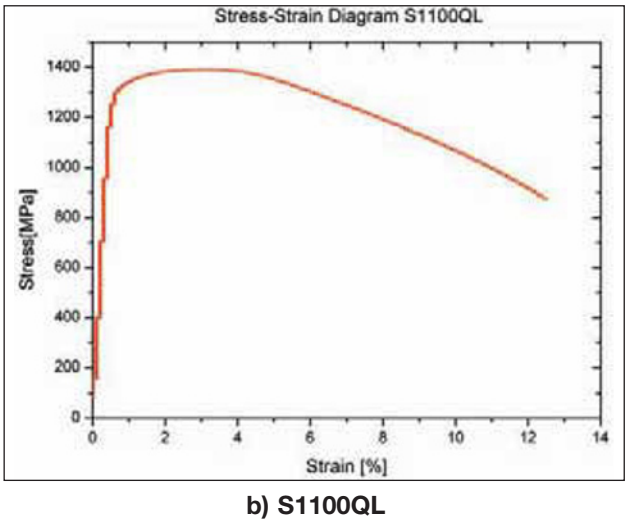

b) S1100QL

Figure 7 – Monotonic stress-strain curve

Table 2 – Mechanical properties of the investigated base materials

	Yield stress [MPa]	Ultimate tensile strength [MPa]	Cyclic yield strength [MPa]	Vickers hardness
S355J2G3	400	550	305	229.2 HV1
S1100QL	1 220	1 400		404.4 HV1
G2Si1	360	440		

of the base metals and also includes the mechanical properties of the filler wire (G2Si1) used for welding the S355J2G3 specimens.

Metallography and hardness measurement

For metallographic purposes, the welded specimens were sliced, polished and etched by Nital 4 % solution. Figure 8 a) shows the cross-section of the weld passes which made the joint and also the difference in the microstructures of the weld zones of the investigated samples. In Figures 8 b)-e), different metallurgical zones in the S355J2G3 welded specimens are focused on more closely. In the base material, a ferritic- pearlitic microstructure is observed, which is also partly observed in the fine grain, heat-affected zone. In the coarse grain, heat-affected zone, a martensite and bainite microstructure is dominant and in the weld metal, a bainite microstructure with martensite needles. In Figure 9 a), a cross-section of a welded S1100QL sample is shown. Figure 9 b) shows the base metal with a bainite and martensite microstructure. In Figure 9 c) and 9 d), the fine grain and coarse grain regions in the heat-affected zone show a microstructure containing ferrite, bainite and martensite. In Figure 9 d), the

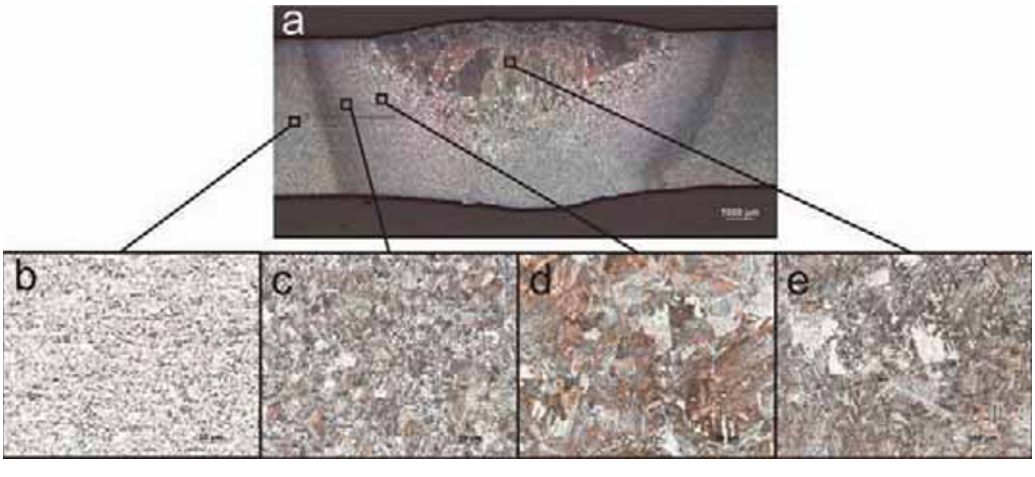

a) Micrograph of the cross-section of a S355J2G3 weld specimen.

Microstructure of different zones of the weld in the b) base material, c) fine grain, heat-affected zone, d) coarse grain, heat-affected zone and e) weld metal

Figure 8

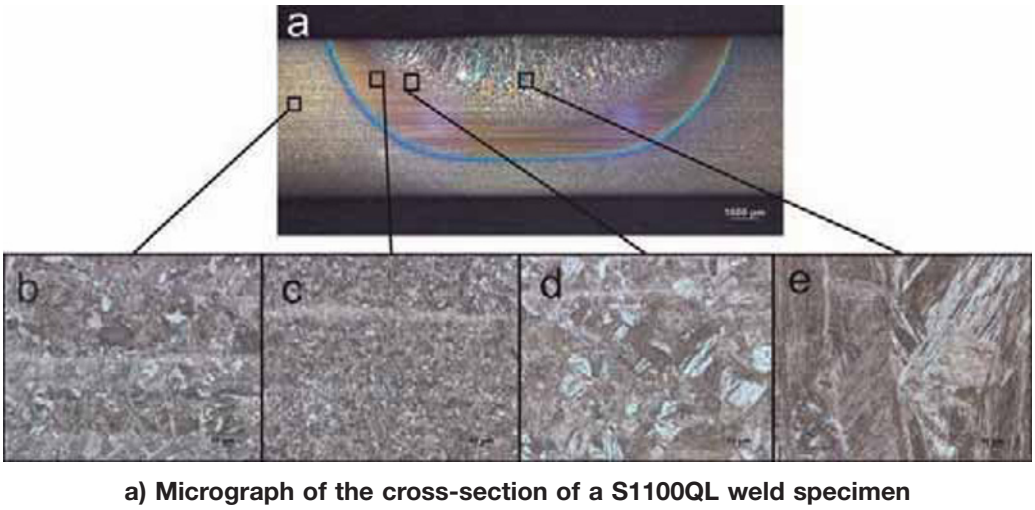

a) Micrograph of the cross-section of a S1100QL weld specimen

Microstructure of different zones of the weld in the b) base material, c) fine grain, heat-affected zone, d) coarse grain, heat-affected zone and e) weld metal

Figure 9

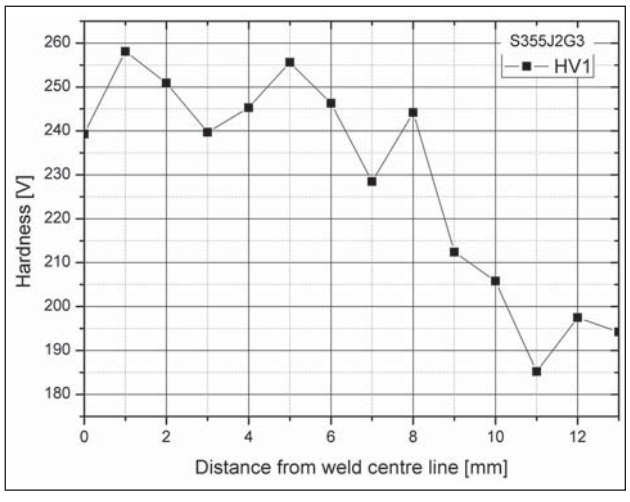

a) S355J2G3

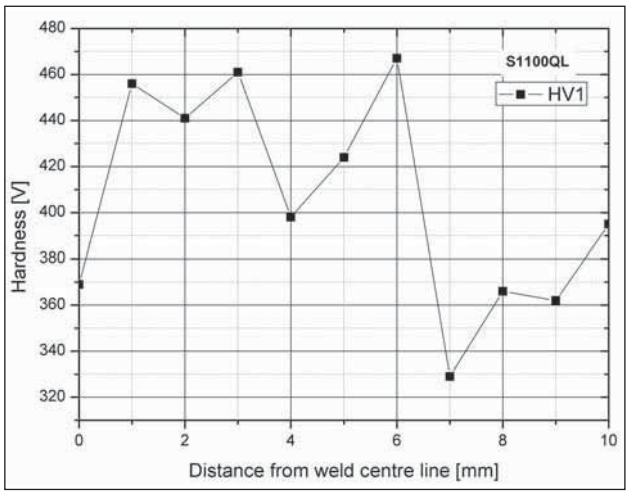

b) S1100QL

Figure 10 – Hardness profile of welded specimens

weld metal with the same microstructure as the heat-affected zone, i.e. ferrite, bainite and martensite, could be observed.

The hardness test was performed with a Zwick 3212 in Vickers scale HV1, according to DIN EN ISO 6507-1.The indented points were placed 1 mm under the surface and at a distance of 1 mm from each other. Figures 10 a) and 10 b) graph the hardness from the weld centre line to the base metal of the welded specimens.

Stress concentration factor calculation and measurement at the weld toe

For studying the stress relaxation in different weld zones, the applied stress in the areas of interest, e.g. weld bead centre line, weld toe and base metal, should be determined. This was done using weld profile measurement, followed by an assessment of the stress concentration factor at the weld toe.

The measurement of the geometry was performed with the help of an indicating calliper with an accuracy of 0.01 mm, moving over the weld bead in 0.1 mm steps and capturing the coordinates of the points on the surface orthogonal to the welding direction [Figure 11 a)]. The scanned geometry was then imported into a finite element program and stress concentration factor at the weld toe was calculated for the position of highest local stress [Figure 11 b)]. The calculated values of stress concentration factors using this method were then compared with stress concentration factors, measured by 3 mm strain gauges (Figure 12). In this experiment, one strain gauge was mounted at the weld toe of the specimen, the weld profile of which had been measured by the calliper and the other strain gauge was installed on the base material 20 mm away from the weld toe. The specimen was loaded with 10 and 20 kN and the strain was measured at the weld and base metal. The strain concentration factor could then be evaluated by dividing the strain measured at the toe, by the strain value at the base material. As the table in Figure 11 shows, the calculated and measured stress concentration factors correlate and a stress concentration factor of 1.3 is determined.

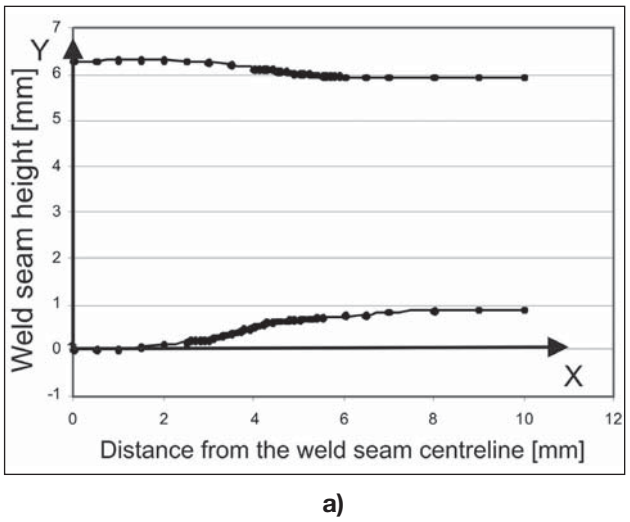

a)

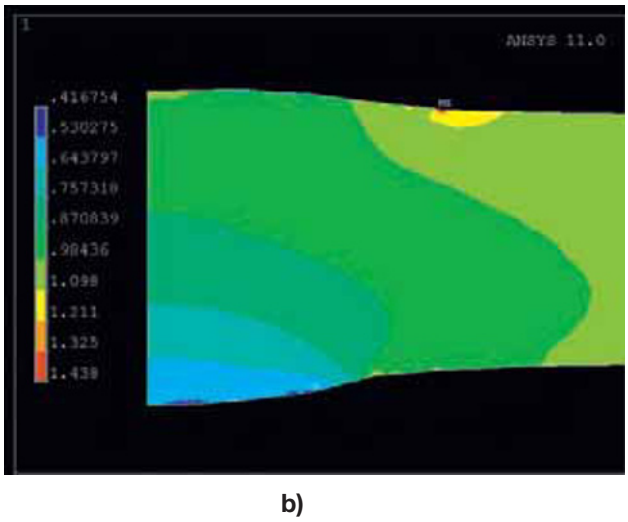

b)

Figure 11 – Weld surface measurement and stress concentration calculation

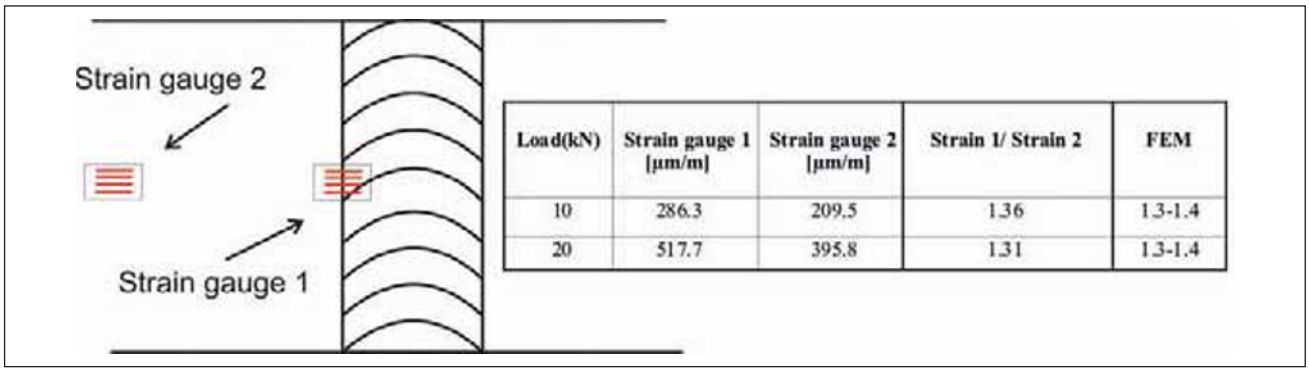

Load(kN)	Strain gauge 1 [μm/m]	Strain gauge 2 [μm/m]	Strain 1/ Strain 2	FEM
10	286.3	209.5	1.36	1.3-1.4
20	517.7	395.8	1.31	1.3-1.4

Figure 12 – Position of the strain gauges for evaluation of strain concentration factors

DISCUSSION

The residual stresses are subjected to the same laws of equilibrium which apply to ordinary stresses produced by external loads. In this study, the residual stress state is considered to be plane stress and the bi-axial residual stress relaxation under axial loading is investigated. The Von Mises failure criterion is used to determine the material limit after which the residual stress relaxes due to plastic deformation. The Von Mises stress, which is a function of transverse and longitudinal residual stresses, load and mean stresses, was calculated for each measured point. In this calculation, the stress concentration factor at the weld toe and the reduction of load stress at the weld beam centre line, due to an increase in weld cross-section, are taken into consideration. The Von Mises stresses at the weld centre line, the weld toe and in the base material under loading until 10^4 cycles were graphed inside the Von Mises yield envelope. Figures 13 a) and 13 b) illustrate the residual stress relaxation in the S355J2G3 specimens for two loading conditions. The graph is divided into three zones:

(I) inside the cyclic yield surface,
(II) between the cyclic and monotonic yield surfaces,
(III) outside the monotonic yield surface.

During the first loading cycle, the Von Mises stress exceeds the monotonic yield strength of the base material at the weld centre line and weld toe. This leads to residual stress relaxation at these two points. The amounts of relaxation at these points are different, depending on the initial residual stress value and actual load stress. In the base material, no relaxation is observed, since the Von Mises stress does not even exceed the cyclic yield strength and stays within the (I) region. For the second loading cycle at the weld centreline and the weld toe, the Von Mises stress exceeds the cyclic yield strength but not the monotonic yield strength. As it is seen, the residual stress does not show any noticeable relaxation and the small circles representing residual stress status are concentrated in one area. This reveals the fact that here the monotonic yield strength is the material resistance against the relaxation. At the weld toe and in the base material, the Von Mises stress does not exceed yield strength. And, as expected, this leads to no residual stress changes.

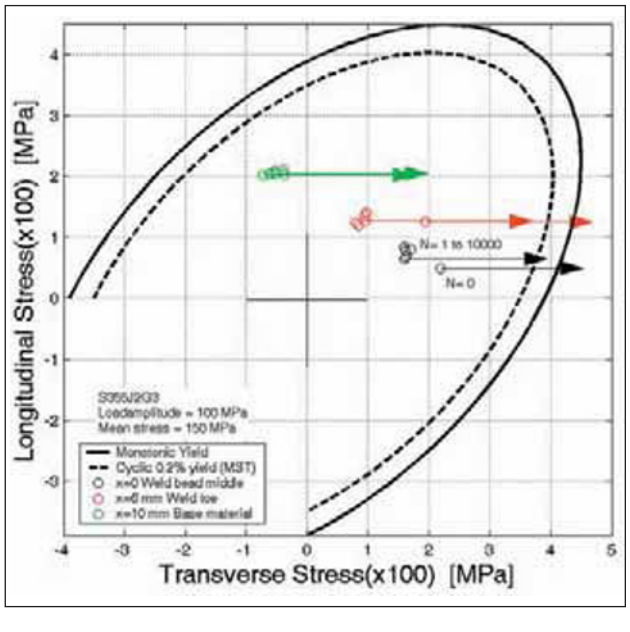

a) Load amplitude 100 MPa

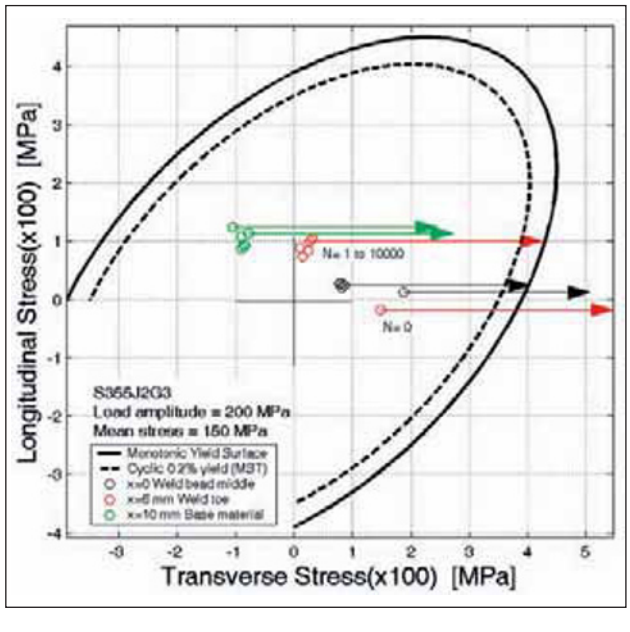

b) Load amplitude 200 MPa

Figure 13 – Residual stress relaxation under cyclic loading, based on Von Mises yield criteria

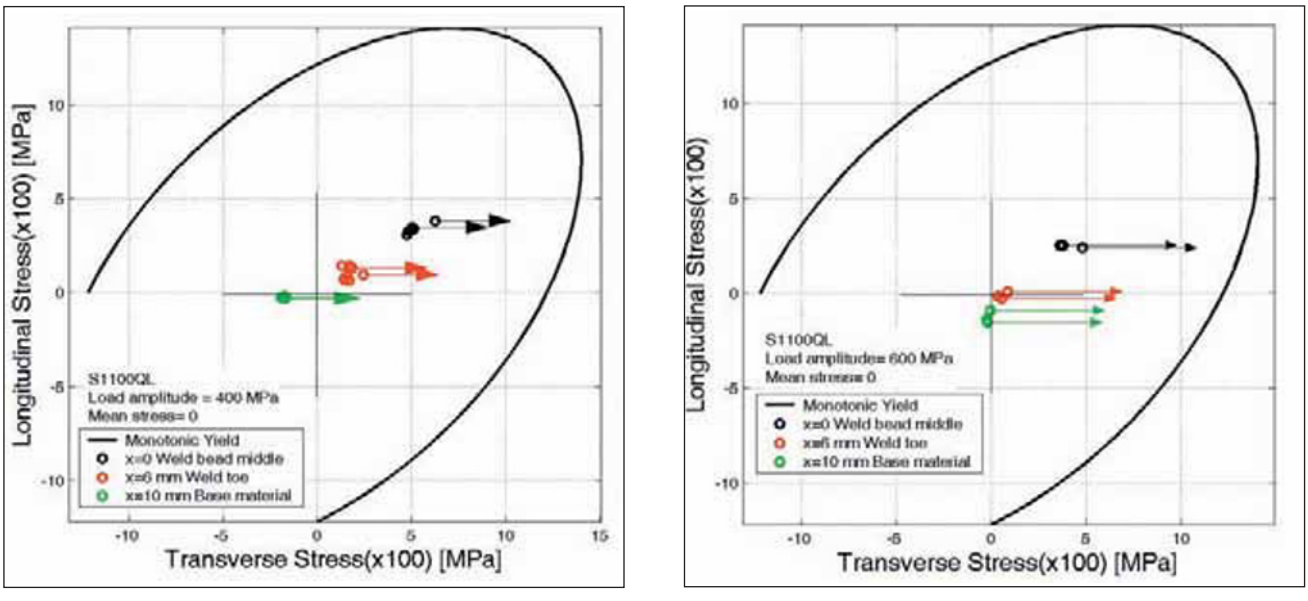

a) Load amplitude 400 MPa **b) Load amplitude 600 MPa**

Figure 14 – Residual stress relaxation under cyclic loading, based on Von Mises yield criteria

For S1100QL, the residual stress relaxation after the first loading in the weld centre line could not be described by the model. The transverse residual stress in the bead centre line for both loading conditions relaxes around 100 MPa (Figure 14), although the monotonic yield strength of the material during loading is not exceeded. The reason could be the relatively incorrect assumption of yield strength similarity throughout the all welding zones. As observed in Figure 10 b), the hardness of the weld centre line (365 HV1) is lower than that of the base material (404 HV1). This could be an indication of relatively lower yield strength of the weld at this point, compared to the base metal, and can explain the unexpected residual stress relaxation at this point. A more systematic material characterization in the welding zones is needed to answer this question.

For the weld toe and base material, it can be seen that no relaxation takes place and the circles representing the residual stress status after loading stay reasonably close to each other in the same area.

CONCLUSION

Residual stress relaxation occurred when the Von Mises stress exceeded the monotonic yield strength in both quasi-static and cyclic loading conditions. In the cyclic loading condition, despite exceeding the cyclic yield strength, no significant residual stress relaxation was observed. In Figure 15, the residual stress relaxation curves in the weld centre line of the S355J2G3 speci-

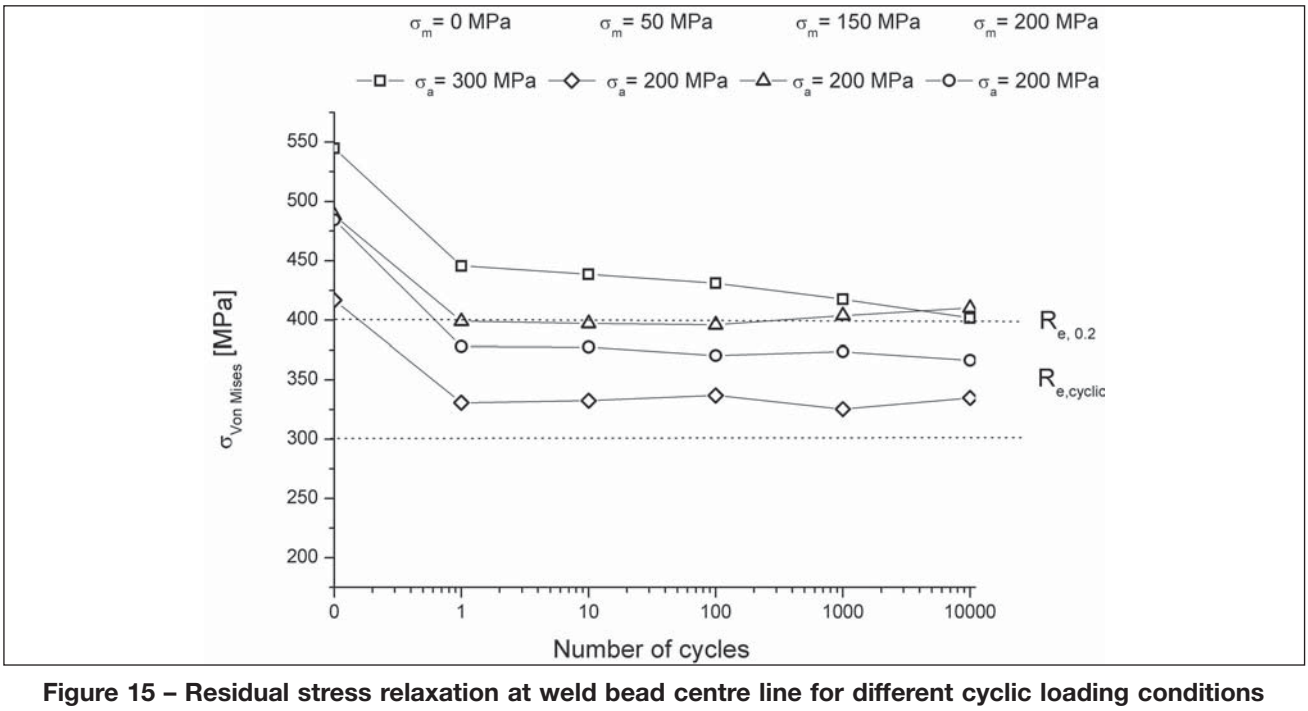

Figure 15 – Residual stress relaxation at weld bead centre line for different cyclic loading conditions of S355J2G3

mens for different load amplitudes and mean stresses are graphed. The two horizontal lines represent the monotonic yield strength $R_{0.2}$ and cyclic yield strength $R_{e,cyclic}$ of the base metal.

As it could be seen after the relaxation during the first cycle, the relaxation continues as long as the Von Mises stress exceeds the monotonic yield strength. That is the case for load amplitude 300 MPa and no mean stress. When the Von Mises stress is below the monotonic yield strength, the residual stresses remain stable and no relaxation occurs. This condition does not depend on the number of load cycles.

In this work, the surface, residual stress relaxation has been studied and in-depth measurement and determination of the residual stress fields are not included. For a comprehensive investigation of the residual stress behaviour, in-depth measurement of the specimens could be of interest.

ACKNOWLEDGEMENTS

The investigations presented were supported by the German Research Foundation (Deutsche Forschungsgemeinschaft – DFG) as part of the project “Residual stress relaxation in welded high-strength steel under cyclic loading.” The authors would like to thank the DFG for its support.

REFERENCES

[1] Ross M.: Experiments for the determination of the influence of residual stresses on the fatigue strength of structures, Welding Research BWRA, 1950, vol. 4, no. 5, pp. 83-93.

[2] Hebrant F., Louis H., Soete W., Winckier A., The relaxation of residual welding stress by static and fatigue loading, Welding Reseach Abroad, 1957, pp. 58-63.

[3] Dugdale D.S.: Effect of residual stress on fatigue strength, Welding Journal, 1959, vol. 38, no. 1, Research supplement, pp. 45-s-48-s.

[4] Maddox S.J., Mantheghi S.: Methods for fatigue life improvements of welded joints in medium and high strength steels, IIW Doc. XIII-2006-04, 2004.

[5] Akihiko O., Yoshio M., Naoyuki S.: Doubled fatigue strength of box welds by Low Transformation Temperature welding wire, Journal of Constructional Steel, 1999, pp. 173-180.

[6] Shiga C., Mraz L., Bernasovsky P., Hiraoka K., Mikula P., Vrana M.: Residual stress distribution of steel welded joints with weld metal of low martensite transformation temperature, Doc. IIW-1824-07 (ex-doc. IX-2149r1-05), Welding in the Word, 2007, vol. 51, no. 1/12, pp. 11-19.

[7] Holzapfel H., Shulze V., Vöhringer O., Macherauch E.: Residual stress relaxation in an AISI 4140 steel due to quasistatic and cyclic loading at higher temperatures, Materials Science and Engineering,1998, A248, pp. 9-18.

[8] Vöhringer O., Wohlfahrt H.: Abbau Von Eigenspanungen, Relaxation of residual stresses, HTM, Zeitschrift für Wärmebehandlung und Werkstofftehnik, Carl Hanser Verlag, 1982, pp. 144-156 (in German).

[9] Zhuang W.Z., Halford G.R.: Investigation of residual stress relaxation under cyclic load, International Journal of Fatigue, 2001, vol. 23, Supplement 1, pp. 31-37.

[10] Mattson R.L., Coleman W.S. Jr.: Effect of shot peening variables and residual stresses on fatigue life of leaf spring specimens, Transactions, Society of Automotive Engineers, 1954, vol. 62, pp. 546-556.

[11] Morrow J., Sinclair G.M.: Cycle-dependent stress relaxation, In: Symposium on basic mechanisms of fatigue, ASTM STP 237, American Society for Testing and Materials, 1958.

[12] Jhansale H. R., Topper T.H.: Engineering analysis of the inelastic stress response of a structural metal under variable cyclic strains, In: Cyclic Stress-Strain Behaviour – Analysis, Experimentation and Failure Prediction, American Society for Testing and Materials, 1973, pp. 246-70.

[13] Vöhringer O.: Abbau Von Eigenspannungen, Relaxation of residual stresses, in: E. Macherauch, V. Hauk (Eds.), Eigenspannungen, Entstehung-Messung-Bewertung (Residual Stresses, Development-Measurement-Evaluation), DGM Informationsgesellschaft, Oberursel, 1983, pp. 49-83 (in German).

[14] Vöhringer O.: Relaxation of residual stresses by annealing or mechanical treatment, in: A. Niku-Lari (Ed.), Advances in Surface Treatments, 1987, vol. 4., International Guidebook on Residual Stresses, Pergamon Press, Oxford, pp. 367-396.

[15] Hoffmann J., Scholtes B, Vöhringer O., Macherauch E.: Thermal relaxation of shot peening residual stresses in differently heat treated plain carbon steel Ck 45, in: H. Wohlfahrt, R. Kopp, O. Vöhringer (Eds.), Proceedings of the International Conference Shot Peening 3, Garmisch-Partenkirchen, 1987, DGM Informationsgesellschaft, Oberursel, 1987, pp. 239-246.

[16] Vöhringer O., Hirsch T., Macherauch E.: Relaxation of shot peening induced residual stresses of TiAl 6 V 4 by annealing or mechanical treatment, in: G. Lütjering, U. Zwicker, W. Bunk (Eds.), Titanium Science and Technology, Proceedings of the 5th International Conference on Titanium, DGM Informationsgesellschaft, Oberursel, 1985, vol. 4, pp. 2203-2210.

[17] Hirsch T., Vöhringer O., Macherauch E.: Der thermische Abbau Von Strahleigenspannungen bei TiAl6V4, The thermal relaxation of shot peening induced residual stresses in TiAl6V4, Härterei-Techn. Mitt., 1983, vol. 38, pp. 229-232 (in German).

[18] Schlaak U., Hirsch T., Mayr P.: Röntgenographische in-situ-Messungen zum thermischen Eigenspannungsabbau bei erhöhter Temperatur, In-situ X-ray measurement of thermal relaxation of residual stress at high temperature, Härterei-Technische Mitteilungen, 1988, 43, pp. 92-102 (in German).

[19] Wiewecke F., Wohlfahrt H., Vöhringer O.: Thermischer Abbau Von Schweißeigenspannungen, Thermal Relaxation of Welding Residual Stresses, Härterei-Technische Mitteilungen, 1990, 45, pp. 293-299 (in German).

[20] Roth M.: Die thermische Stabilität Von Eigenspannungen in kugelgestrahlten Oberflächen, Thermal stability of residual stresses in shot peened surfaces, Z. Werkstofftechnik, 1987, 18, pp. 225-228 (in German).

[21] Masmoudi N., Castex L.: The effect of temperature and time on the stress relaxation of shot peened nickel base superalloy IN 100, in: G. Beck, S. Denis, A. Simon (Eds.), Proceedings of the 2nd International Conference on Residual Stresses, Nancy, 1988, Elsevier, Amsterdam, 1989, pp. 710-715.

[22] Hanagarth H.: Auswirkung Von Oberflächenbehandlungen auf das Ermüdungsverhalten Von TiAl 6 V 4 und 42 CrMo 4 bei erhöhter Temperatur, The influence of surface treatment on fatigue behavior of TiAl6V4 and 42 CrMo4 at high temperature, Dr.-Ing.-Diss., Universität Karlsruhe (TH), 1989 (in German).

[23] Hirsch T., Vöhringer O., Macherauch E.: Der Einfluß Von Zug-bzw. Druckverformungen auf die Oberflächeneigenspannungen Von gestrahltem AlCu 5 Mg 2, The influence of tension and compression on surface residual stresses of shot peened AlCu5 Mg2, Härterei-Technische Mitteilungen, 1988, 43, pp. 16-20 (in German).

[24] Hanagarth H, Vöhringer. O, Macherauch. E, Relaxation of Shot Peening Residual Stresses of the Steel 42 CrMo 4 by Tensile or Compressive Deformation, in: K. Iida (Ed.), Proceedings of the International Conference Shot Peening 4, Tokyo, 1990, The Japan Society of Precision Engineering, Tokyo, 1990, pp.337-345.

[25] Schulze V.: Die Auswirkungen kugelgestrahlter Randschichten auf das quasistatische sowie ein- und zweistufige zyklische Verformungsverhalten Von vergütetem 42CrMo 4, The influence of shot peened surfaces on quasi-static and cyclic deformation in 42CrMo 4, Dr.-Ing.-Dissertation, Universität Karlsruhe (TH), 1993 (in German).

[26] Kirk D.: Effects of plastic straining on residual stresses induced by shot peening, in: H. Wohlfahrt, R. Kopp, O. Vöhringer (Eds.), Proceedings of the International Conference Shot Peening 3, Garmisch- Partenkirchen, 1987, DGM Informationsgesellschaft, Oberursel, 1987, pp. 213-220.

[27] Cammet J. T., Sauer C.A., Arnold T.E.: Observations on shot peening residual stresses in 17Cr-7Ni austenitic stainless steel and their redistribution via mechanical loading, in: D. Kirk (Ed.), Proceedings of the International Conference Shot Peening 5, Oxford, 1993, Coventry University, 1994, pp. 282-289.

[28] Schulze V., Lang K.H., Vöhringer O., Macherauch E.: Relaxation of shot peening induced residual stresses in quenched and tempered steel AISI 4140 due to uniaxial cyclic deformation, in: J. Champaigne (Ed.), Proceedings of the 6th International Conference on Shot Peening, San Francisco, 1996, pp. 403-412.

[29] Kodama S.: The behaviour of residual stress during fatigue stress cycles, in: Proceedings of the International Conference on Mechanical Behaviour of Metals, vol. 2, Society of Material Science press, Kyoto, 1972, pp. 111-118.

[30] Wohlfahrt H.: Shot peening and fatigue of materials, in: A. Niku-Lari (Ed.), Proceedings of the International Conference Shot Peening 1, Pergamon Press, Oxford, 1982, pp. 675-694.

[31] Bergström J.: Relaxation of residual stresses during cyclic loading, in: A. Niku-Lari (Ed.), Advances in Surface Treatments, Technology-Application-Effects, 1986, vol. 3, Pergamon Press, New York, pp. 55-62.

[32] Leverant G.R., Langer B.S., Yuen A., Hopkins S.W.: Surface residual stresses, surface topography and the fatigue behavior of Ti-6Al-4V, Metallurgical Transactions,1979, 10A, pp. 251-257.

[33] Hoffmann J.E.: Der Einfluß fertigungsbedingter Eigenspannungen auf das Biegewechselverhalten Von glatten und gekerbten Proben aus Ck 45 in verschiedenen Werkstoffzuständen, The influence of process induced residual stresses on bending fatigue behaviour of flat and notched Ck 45 specimens in difference material status, Dr.-Ing.-Dissertation, Universität Karlsruhe (TH), 1984 (in German).

[34] Boggs B.D., Byrne J.G.: Fatigue stability of residual stress in shot peened alloys, Metallurgical and Materials Transactions B, 1973, vol. 4, no. 9, pp. 2153-2157.

[35] James M.R., Morris W.L.: Fatigue changes in surface residual stress, Scripta Metallurgica, 1983, 17, pp. 1101-1104.

[36] Meguid S.A., Hammond D.W.: Fatigue fracture and residual stress relaxation in shot peened components, in: G. Beck, S. Denis, A. Simon (Eds.), Proceedings of the 2nd. International Conference on Residual Stresses, Nancy, 1988, Elsevier, Amsterdam, 1989, pp. 797-802.

[37] Morrow J., Ross A.S., Sinclair G.M.: Relaxation of residual stresses due to fatigue loading SAE Trans., 1960, 68, pp. 40-48.

[38] McClinton M., Cohen J.B.: Changes in residual stress during the tension fatigue of normalized and peened SAE 1040 steel, Materials Science and Engineering, 1982, 56, pp. 259-263.

[39] Smith D.J., Farrahi G.H., Zhu W.X., McMahon C.A.: Experimental measurement and finite element simulation of the interaction between residual stresses and mechanical loading, International Journal of Fatigue, 2001, vol. 23, no. 4, pp. 293-302.

[40] Macherauch E., Müller P.: Das $\sin^2\Psi$-Verfahren der röntgenographischen Spannungsmessung, The $\sin^2\Psi$ method in x-ray stress analysis, Zeitschrift. Angew. Phys., 1961, 13, pp. 305-312 (in German).

[41] Hauk V.: Structural and residual stress analysis by nondestructive methods, Elsevier Science B.V., ISBN: 0 444 82476 6, 1997.